Direct observation of an ensemble of stable collapsed states in the mechanical folding of ubiquitin

Sergi Garcia-Manyes[a,1], Lorna Dougan[a,2], Carmen L. Badilla[a], Jasna Brujić[b], and Julio M. Fernández[a,1]

[a]Department of Biological Sciences, Columbia University, New York, NY 10027; and [b]Department of Physics, Center for Soft Matter Research, New York University, New York, NY 10003;

Edited by Peter G. Wolynes, University of California at San Diego, La Jolla, CA, and approved May 12, 2009 (received for review February 3, 2009)

Statistical theories of protein folding have long predicted plausible mechanisms for reducing the vast conformational space through distinct ensembles of structures. However, these predictions have remained untested by bulk techniques, because the conformational diversity of folding molecules has been experimentally unapproachable. Owing to recent advances in single molecule force-clamp spectroscopy, we are now able to probe the structure and dynamics of the small protein ubiquitin by measuring its length and mechanical stability during each stage of folding. Here, we discover that upon hydrophobic collapse, the protein rapidly selects a subset of minimum energy structures that are mechanically weak and essential precursors of the native fold. From this much reduced ensemble, the native state is acquired through a barrier-limited transition. Our results support the validity of statistical mechanics models in describing the folding of a small protein on biological timescales.

force-clamp spectroscopy | protein folding

More than 2 decades ago statistical theories of protein folding, developed from simplified models of proteins (1) and scaling laws borrowed from polymer physics (2), offered an appealing framework for how proteins fold (3–5). These pioneering studies laid down the foundation of the "new view" of the protein folding theory (6–8). From this viewpoint, a polypeptide exposed to folding conditions is thought to go through progressively smaller conformational ensembles along a rough, funnel-like energy surface leading to the native state topology (8, 9). The envisaged stages of folding involve an initial hydrophobic collapse into a large set of nonspecific globular structures, which then select a few minimum energy collapsed conformations that fold via activated all-or-none transitions (4, 5, 10–14). Time scales for each one of these phases were estimated from simplified models to range from microseconds for the collapse to seconds for the final fold (2, 12). Although theoretical models propose physical mechanisms underlying protein folding (12, 15–17), their experimental verification has been inaccessible. Observing the multitude of trajectories and folding structures using bulk techniques averages out the ensembles predicted by the statistical theories of protein folding. Much of the literature studying bulk denaturation and refolding of proteins therefore reports 2-state folding reactions where even the presence of single folding intermediates is controversial (18, 19). Indeed, as pointed out by Dill and Chan (15) in their seminal review, the predictions made by the statistical theories are in conflict with the view that folding proceeds through a well defined pathway that crosses a single energy barrier to the native state. This longstanding debate can only be addressed by sampling the conformational diversity of a single protein along its folding trajectory.

Here, we demonstrate that single protein force-clamp spectroscopy using the AFM captures the diversity of the collapsed conformations and their time scales, which are necessary to evaluate the scenario for protein folding (20, 21). In our experiments, the protein is first extended to a well-defined state and its subsequent journey to the native conformations is then monitored as a function of the protein length over time (20–23). By mechanically perturbing the ensembles that form along the folding trajectories, we gain insights into their role in folding (24). A crucial component of the statistical theories of protein folding was the existence of a reduced ensemble of minimum energy collapsed conformations that were thought to play a key role in reducing the dimensionality of the search for the native basin (10–13). Our experiments demonstrate the existence of this ensemble and the key role that it plays in folding. Our observations directly confirm the predictions made by statistical theories of folding, and demonstrate a unique experimental approach for an in-depth exploration of the folding energy landscape of a protein, a central problem in biology.

Results and Discussion

Using the AFM in the force-clamp mode, we have shown the ability to observe unfolding and refolding trajectories of single polyprotein molecules (20, 22). A single polyubiquitin was first mechanically unfolded and extended at a high force of 110 pN (Fig. 1*A*), resulting in a series of length steps of 20 nm. The repeating steps serve as a signature of the natively folded protein. Each step marks the release of 61 aa (25), trapped behind the mechanical transition state located between the β1-β5 strands (26). Quenching to a low force of 10 pN triggers the collapse of the extended polypeptide, followed by refolding to the mechanically stable native state (20). Here, we expand our previous observations by varying the time that the protein is held at the low force, Δt, to probe the structures sampled by the refolding protein (24). Recovery of mechanical stability of the proteins then serves as a signature of their native-like character. A test pulse back to a high force of 110 pN measured the resulting unfolding kinetics for each Δt. As shown in Fig. 1*A*, the unfolding kinetics of the same molecule depends on Δt, such that after a short quench (100–200 ms) the subsequent test pulse results in fast unravelling of the polypeptide and an absence of 20-nm unfolding steps. As Δt increases to 500 ms, these steps become detectable, whereas after 3 s they are predominant. This behavior qualitatively captures the kinetics of refolding. By systematically varying Δt between 0.2 and 15 s (Fig. 1*B*) for an average of 30–60 individual trajectories, we quantified the unfolding rate kinetics of the conformational states visited along the folding process (24).

A 2-state model of folding would imply an all-or-none transition to the folded state, resulting in the observation of either no mechanical stability of the collapsed protein, or the same rate

Author contributions: S.G.-M. and J.M.F. designed research; S.G.-M., C.L.B., and L.D. performed research; C.B.-F. contributed new reagents/analytic tools; S.G.-M., L.D., and J.M.F. analyzed data; and S.G.-M., L.D., J.B., and J.M.F. wrote the paper.

The authors declare no conflict of interest.

This article is a PNAS Direct Submission.

[1]To whom correspondence may be addressed. E-mail: jfernandez@columbia.edu or sergi@biology.columbia.edu.

[2]Present address: School of Physics and Astronomy, University of Leeds, Leeds, LS2 9JT.

This article contains supporting information online at www.pnas.org/cgi/content/full/0901213106/DCSupplemental.

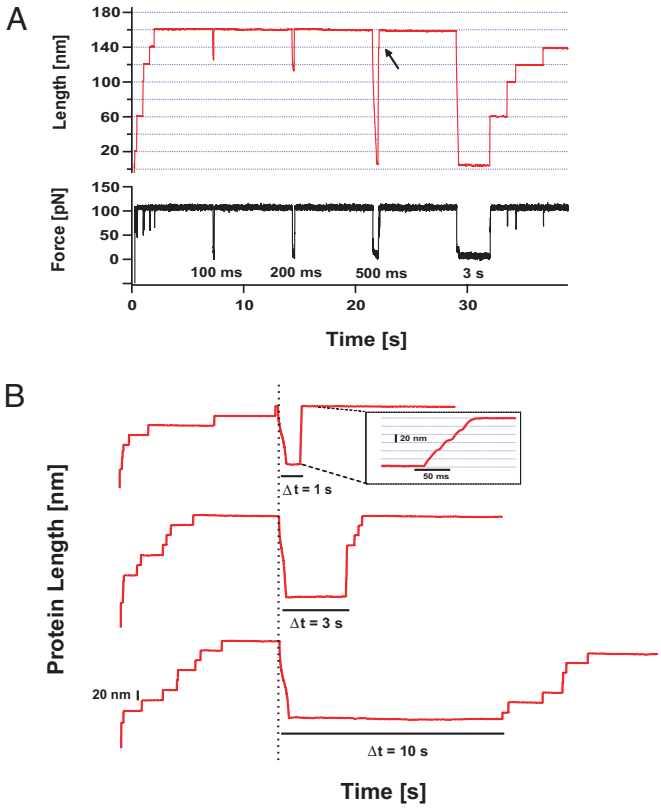

Fig. 1. Identification of a weakly stable ensemble of collapsed conformations in the folding of ubiquitin. (*A*) We repeatedly unfold and extend a ubiquitin polyprotein at 110 pN and then reduce the force to 10 pN for a varying amount of time, Δt, to trigger folding. First the polyprotein elongates in well defined steps of 20 nm, because each protein in the chain unfolds at a high force. Upon quenching the force the extended protein collapses. We probe the state of the collapsed polypeptide by raising the force back to 110 pN and measuring the kinetics of the protein elongation. (*B*) After full collapse we observe that the protein becomes segregated into 2 distinct ensembles: The first is identified by a fast heterogeneous elongation made of multiple sized steps (*Inset*); the second corresponds to well defined steps of 20 nm that identify fully folded proteins. The ratio between these 2 states of the protein depends on Δt. Longer values of Δt favor the native ensemble.

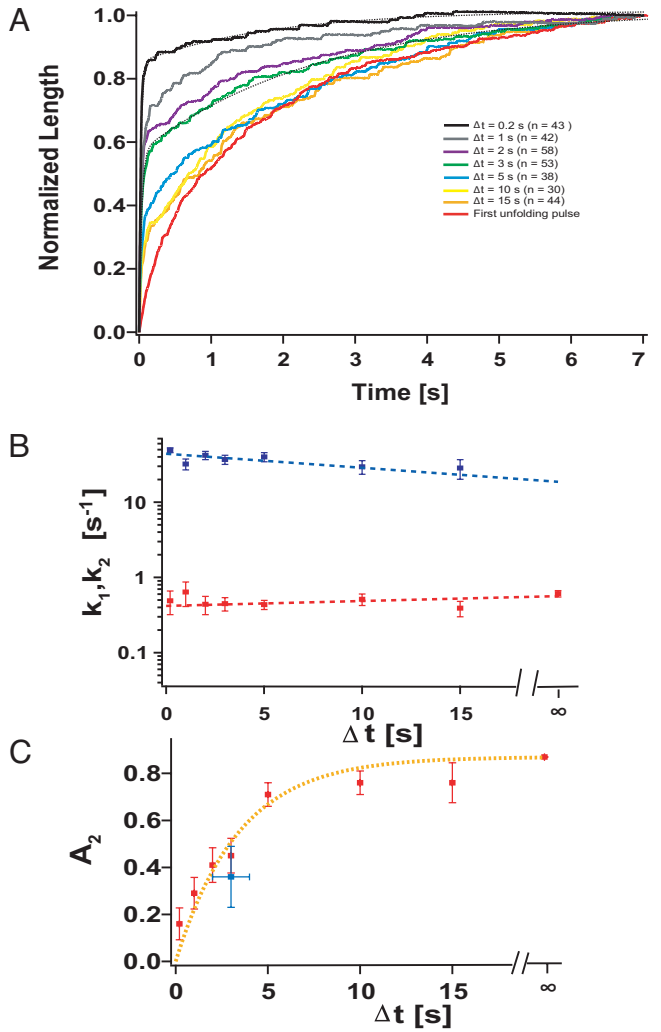

Fig. 2. Kinetics of conversion from collapsed to native conformations. Extended proteins were allowed to collapse for a duration Δt, and then were reextended at a high force to probe the nature of the collapsed ensemble. (*A*) For a given Δt, averages of 30–60 extensions are well described by double exponential fits (dotted lines). The fits measure the unraveling rate constant of the weakly stable collapsed state, k_1, and the fully stable protein, k_2, and their relative amplitude A_1 and A_2. (*B*) k_1 is 40-fold faster than k_2, while both are nearly independent of Δt (blue and red squares, respectively). The rate $k_2 = 0.5\,s^{-1}$ is in close agreement with the kinetics of unfolding of native ubiquitin. (*C*) The fraction of native conformations, A_2, increased exponentially with Δt (dotted line) with a rate constant of $k_f = 0.3\,s^{-1}$. The blue data point highlights that the formation of native contacts occurs only after the folded length is reached (*SI Appendix*, Fig. S2).

kinetics as the initial unfolding staircase. Instead, we capture 2 distinct phases; a fast initial extension that unravels the collapsed states in a stepwise manner featuring different lengths (Fig. 1*B Inset* and *SI Appendix*, Fig. S1) followed by a much slower staircase of 20-nm steps, characteristic of fully refolded ubiquitin.

Normalized ensemble averages of protein length over time from 308 refolding polyproteins are shown in Fig. 2*A*, obtained for each Δt. In all cases, the time course of polyprotein extension was well described by a double exponential fit. This fit corresponds to a fast phase (phase 1) and a slow phase (phase 2). The rate constants for each phase, k_1 and k_2, show almost no dependence on Δt in Fig. 2*B*, suggesting that the protein does not gradually progress from higher to lower energy states, but populates 2 distinct conformational states. The rate constant k_1 is 40 times faster than the slow phase, characteristic of a mechanically weak structure. The slow phase exhibits the same rate constant, $k_2 = 0.5 \pm 0.1$s, as the natively folded protein (see Fig. 4*B*). The amplitude of the latter phase, A_2, which corresponds to the folded fraction, increased exponentially with waiting time, Δt, at a rate of $0.3\,s^{-1}$ (Fig. 2*C*). In our experiments, we quench the force to a low value (10 pN) such that the protein reaches the collapsed state in a short time (<100 ms). However, in a few cases the trajectories took longer to collapse (*SI Appendix*, Fig. S2). For those cases, the folded fraction (Fig. 2*C*) corresponds to a value of Δt measured from the time when full collapse was reached, which was shorter than the duration of the quench. The blue symbol in Fig. 2*C* demonstrates this point. The exponential recovery shown in Fig. 2*C* indicates that the conversion from the mechanically weak collapsed states into the native conformations occurs through a barrier-activated process (24, 27).

Stepwise unfolding under force-clamp conditions is the signature of a barrier crossing event where a protein unravels and extends in an all-or-none manner, as seen in Fig. 3*A*. The size of the step increase in length, ΔL, is a measure of the number of amino acids behind the transition state of the protein (25). In the case of a folded ubiquitin the position of the transition state is well defined (26), giving rise to a narrow distribution of step sizes

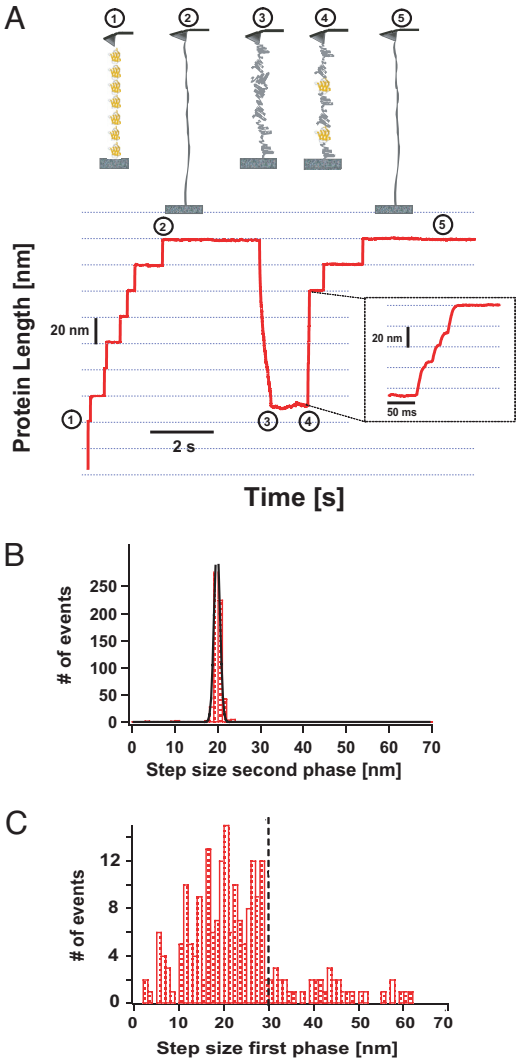

Fig. 3. A broad ensemble of transition states characterizes the collapsed conformations. The test pulse in a typical refolding trajectory of a single polyubiquitin protein with a short collapse time Δt is composed of 2 distinct regimes. In both regimes the polyprotein elongates in a stepwise manner. A stepwise extension under force identifies a conformation that extends by overcoming an energy barrier (*A*). The precise location of the transition state within the structure determines the number of amino acids that will extend after the barrier is crossed. The native state is marked by stepwise extensions that are narrowly distributed around 20 nm 19.7 ± 0.6 nm ($n = 607$) (*A* and *B*), signifying a well defined transition state. By contrast, the majority of the collapsed conformations extend in steps that cover a wide range of values up to 29 nm, with a reduced number as high as 62 nm (*C* and *A Inset*). The distribution of step sizes of the collapsed conformations is largely contained within the contour length of a single ubiquitin monomer (dashed line in *C*). The observation of individual collapsed states is limited to the time resolution of our feedback response, 5–10 ms.

(ΔL = 19.7 ± 0.6 nm, Fig. 3*B*). By contrast, unraveling the collapsed states features a broad distribution of step sizes spanning from 1 nm all of the way to 62 nm (Fig. 3*C*). The majority (≈88%) of the measured step sizes lie below ≈29 nm (dashed line in Fig. 3*C*). The theoretical limit of length increase that one could observe by extending a collapsed ubiquitin polypeptide is 30.4 nm (76 aa × 0.4 nm per amino acid (25). This maximal contour length increase would correspond to unraveling a hypothetical collapsed state that had a single bond placed between the first and last residues in the polypeptide. Scaled by the WLC model of polymer elasticity, this would result in a maximal step increase in length of 29 nm at a pulling force of 110 pN (*SI Appendix*, Fig. S3*A*). Therefore, the measured distribution of step sizes of the collapsed conformations shown in Fig. 3*C* is largely contained within the contour length of a single ubiquitin monomer (dashed line in C). Although a precise quantification of the number of states in the collapsed ensemble is difficult to extract from our data (28), the heterogeneity in the measured step sizes suggests that the weak mechanical conformations exhibit transition states that can occur anywhere within the structure (*SI Appendix*, Fig. S3*B*). A small number of larger step sizes (≈12%) were also observed, because of either a lack of sufficient time resolution or conformations that involved 2 neighboring ubiquitins. Remarkably, the distribution of step sizes does not significantly evolve with Δt (*SI Appendix*, Fig. S4), suggesting that the ensemble of collapsed states might exhibit static disorder. In this scenario, each particular collapsed state would hop into a particular native state conformation independently, which might explain the broad distribution of mechanical stabilities observed in the native state (29) .

The existence of such an ensemble of collapsed states (Fig. 3 *A*–*C*) may be a general feature of proteins that are naturally designed through evolution to fold on biological timescales (30). Indeed, we have experimentally observed a similar ensemble of collapsed states in the 27th Ig module of the giant protein titin, both in its polyprotein and monomeric forms (*SI Appendix*, Figs. S5 and S6). As a negative test of this hypothesis, we have examined the collapsing behavior of an intrinsically disordered protein, the PEVK region of titin. Owing to the featureless properties of this elastomer (31) we designed a construct containing an I27 fingerprint that allowed us to unambiguously recognize that we had effectively stretched and collapsed the PEVK sequence (32). Our force-clamp data shows that the PEVK polypeptide, unlike ubiquitin and I27, does not form any mechanically resistant collapsed structures (*SI Appendix*, Fig. S6 *B* and *C*).

Probing the force-dependent unfolding rate of native proteins measures important features of the energy landscape, such as the height of the activation energy barrier, ΔG, and the position of the transition state Δx (22, 33). We first characterize the energy barriers associated with the collapsed conformations (Fig. 4*A*). After a collapse of 1 s to the folded length, we pull the proteins at different forces and measure the time course of unraveling them (F_3 in Fig. 4*A*). As a first approximation, we measure the average rate of unraveling corresponding to the full ensemble of collapsed states, despite their structural disorder shown in Fig. 3*C*. Fig. 4*B* shows a logarithmic plot of the average rate of unraveling of the collapsed conformations (triangles) as a function of the pulling force. Although at high forces the data were well described by a single exponential, at lower forces the time course of extension of the collapsed conformations was more complex. We fit the force-dependency of the unraveling rate with a simple Arrhenius term, $k_1(F) = k_{0,1}\exp(F\Delta x_1/k_BT)$, where F is the pulling force, $k_{0,1}$ = 0.7 s^{-1} is the unraveling rate in the absence of force and Δx_1 = 2.0 Å, the distance to the transition state. Assuming a prefactor value (34) of $A = 10^6$ s^{-1} and $k_{0,1} = A\exp(-\Delta G_1/k_BT)$, we calculate an average activation energy of $\langle\Delta G_1\rangle \approx$ 8.4 kcal/mol. Similarly, experiments on the force-dependency of the unfolding rate of natively folded ubiquitin (circles in Fig. 4*B*) give an activation energy of $\Delta G_2 \approx$ 11.0 kcal/mol, and a distance to the transition state of Δx_2 = 1.6 Å (dotted black line), in close agreement with earlier experiments (22, 33). The phenomenological Arrhenius/Bell model applied here relies on the assumption of a force-independent transition state location. Moreover, the estimate for the barrier height is based on assuming a value for the prefactor, A. By contrast, using an alternative approach derived from Kramers's theory in one dimension allows estimation of the distance to the transition state, the unfolding rate in the absence of force and the height

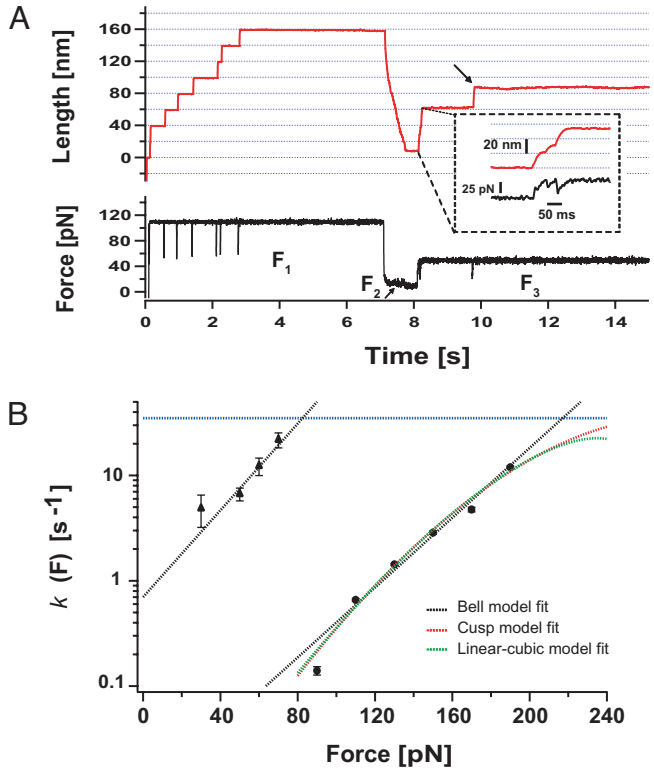

Fig. 4. The collapsed conformations are mechanically labile and exhibit a distance to the transition state similar to that of the native form. We use a 3-pulse protocol (F_1 to F_3 in *A*) to measure the force-dependent extension of both the collapsed and native conformation ensembles. After a standard force-quench sequence (F_1 and F_2), the force-dependent rate of extension of the collapsed conformations k_1 is measured by varying the force of F_3 within the range 30–70 pN, whereas the force dependent rate of unfolding of the native conformations, k_2, is studied by varying F_1 within the range 90–190 pN. Remarkably, the time-course of unraveling the ensemble of collapsed states when pulled at $F_3 = 50$ pN is greatly slowed down, taking place in ≈2 s in this particular trajectory. The length trace corresponding to the force pulse F_3 captures only the unraveling trajectories of individual collapsed states as revealed by their different unraveling step sizes (the last step in the recording at ≈10 s, marked with an arrow, features ≈25 nm) and to the vanishingly small probability of observing a step corresponding to the unfolding of the native state when ubiquitin is pulled at 50 pN. (*B*) A logarithmic plot of the average rate of unraveling of the collapsed conformations (triangles) as a function of the pulling force. These rates were measured from the weighted average of biexponential fits to the unraveling time course of 25–50 recordings at each force (*SI Appendix*, Fig. S8*A*). We fit an Arrhenius term to the unraveling rate of the collapsed conformations $k_1(F)$ (triangles) to estimate the average size of the activation energy barrier, $\langle \Delta G_1 \rangle$, and distance to the transition state, Δx_1, of the collapsed conformations in PBS solution, yielding a $\Delta x_1 \approx 0.2$ Å. To describe the rate of unfolding of the native state (k_2) we use single exponential fits to the average time-course of unfolding at each particular force as a practical first approximation (*SI Appendix*, Fig. S8*B*). As we have demonstrated before, a single exponential fit captures ≈81% of the unfolding events and thus represents a reasonable measure of the unfolding rate (45). Fitting the Arrhenius term to the unfolding rate of the native state $k_2(F)$ (circles) yields a similar distance to the transition state, $\Delta x_2 = 1.6$ Å (dotted black line). Red and green dotted lines correspond to the fit of the experimental data to the analytical equation derived from Kramers's theory (35) assuming a cusp-like and a linear-cubic energy profile, respectively (*SI Appendix*, Table S1). The blue horizontal line represents the limit in the rate resolution for experiments conducted with cantilevers with a spring constant of 15 pN/nm.

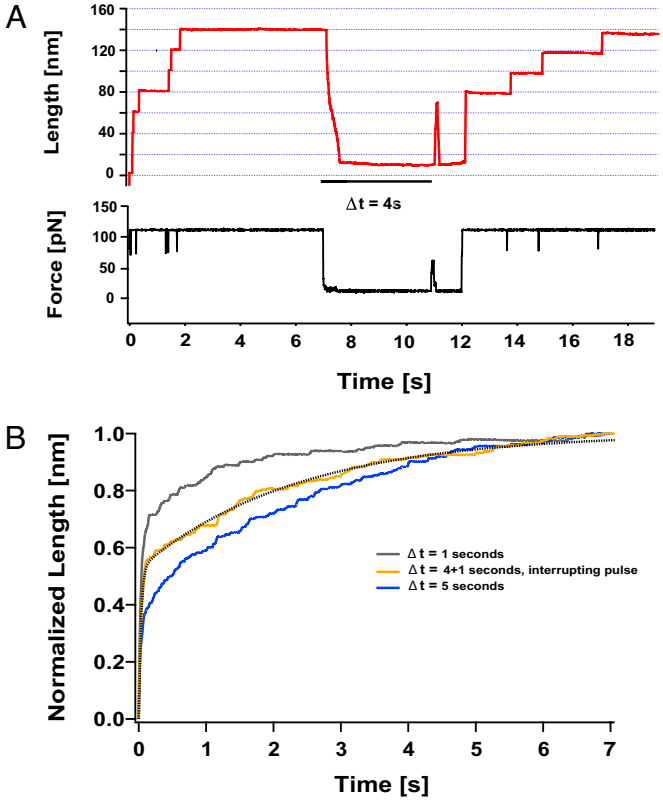

Fig. 5. Collapsed conformations are necessary precursors of the native state. (*A*) After a regular force-quench, we use a brief force pulse (60 pN; 100 ms) to disrupt the ensemble of collapsed conformations during their conversion to the native ensemble. (*B*) We averaged 51 extensions at 110 pN after the interruption of the refolding process at $\Delta t = 4$s (orange) and compared its effect to the average extension time-course obtained for uninterrupted $\Delta t = 5$ s (blue) and $\Delta t = 1$ s (gray) trajectories. It is clear that the short force pulse delays the recovery of the mechanically stable native conformations.

of the energy barrier independently, without the need to rely on an assumption for the prefactor (35). We use the analytical general equation proposed by Dudko et al. (35) (see *SI Appendix*, *SI Text*) to fit the force-dependent unfolding rate of the native state of ubiquitin (Fig. 4*B*) for a free-energy profile corresponding to a harmonic well with a cusp-like barrier (dotted red line) for a potential that contains linear and cubic terms (dotted green line). The values corresponding to Δx_2, $k_{0,2}$, and ΔG_2 obtained for each model are included in the *SI Appendix*, Table S1. According to the limited range of forces (90–190 pN) for which experimental data are available, it is difficult to unambiguously distinguish which of the 3 proposed models captures more precisely the experimental trend. In any case, it is remarkable that the distance to the transition state corresponding to the unfolding of the native state obtained with the 3 different models, $\Delta x \approx 2$ Å, is similar to the value measured for the ensemble of collapsed states. These observations suggest that the interactions setting the free energy of the collapsed states have a similar length scale as those in the native fold.

Although the presence of a set of distinct mechanically weak collapsed conformations is clearly revealed by the preceding experiments, the question remains whether these structures represent necessary folding precursors or unproductive kinetic traps in the folding energy landscape. It is feasible that the refolding events that we observe (e.g., Fig. 1) result from a 2-state folding mechanism, whereas the labile collapsed conformations are a set of misfolded structures away from the main folding pathway. We therefore devised a protocol to disrupt these collapsed conformations by interrupting the folding trajectories with a brief (100 ms) pulse to a higher force of 60 pN (Fig. 5*A*). During such a brief pulse, native ubiquitin has a very low probability of unfolding. The unfolding rate of ubiquitin at 60 pN is ≈0.15 s^{-1} (33). Thus, during a 100 ms pulse we expect

0.015 native ubiquitin unfolding events, which is negligible compared with the high rate of unraveling of the collapsed conformations at this force (~120 s^{-1}; Fig. 4*B*). As a further proof that we are indeed unraveling the ensemble of collapsed states we observe that the stepwise elongation concomitant with the force pulse matches the length distribution characteristic of the minimum energy collapsed states observed in Fig. 3*C* (*SI Appendix*, Fig. S7). If the set of mechanically labile collapsed conformations are a prerequisite to folding, their disruption would cause a delay in the recovery of mechanical stability as compared with the unperturbed trajectories. By contrast, if the collapsed states represent unproductive traps, then unraveling them would accelerate the rate of folding. In Fig. 5*B* we show that an average unfolding trajectory after 5 s of folding has a higher content of folded proteins than the same trajectory with the mechanical interruption. This experiment shows that the collapsed conformations are necessary precursors of the folded state.

Protein folding has been studied using single molecule techniques revealing complex behavior that is difficult to reconcile with the widely accepted 2-state folding scenario. For example, Förster resonance energy transfer (FRET) experiments have allowed decoupling of the polypeptide collapse from folding (36), characterization of the unfolded state of proteins (37) and revealing signatures of conformational heterogeneity along individual folding trajectories (38). However, the limited bandwidth of these experiments (37) places limitations on the detection of complete single protein folding trajectories. Using mechanical force to control the folding status of a protein offers some very significant advantages in that force slows down folding exponentially, thus allowing ample time for the study of complete individual folding trajectories. The ability to precisely control forces of a few pico-Newtons was recently applied to study the refolding properties of proteins such as ddFLN4 and RNase H. Pulling on ddFLN4 with constant-velocity AFM resulted in a well-defined intermediate under a loading force and the absence of a thermodynamically distinct collapse state before final folding occurred (39). By contrast, stretching RNase H protein, using optical tweezers, showed the presence of a weakly stable collapsed folding intermediate (40). This folding intermediate was identified as a "molten globule" state, in accord with the metastable thermodynamic state that is most often used to describe the collapsed states of a folding protein (41). The concept of a "molten globule" as a thermodynamic state that is mostly structured and native-like shares similarities with the minimum energy collapsed states that we report (16, 42). However, the collapsed ensemble that we observe does not correspond to a well defined state.

In the present study we have taken advantage of the versatility of the single molecule force-clamp technique to separate the distinct stages of the folding process of ubiquitin, characterized by substates belonging to the extended, collapsed and native state ensembles in each individual molecule. From the unfathomably large number of conformations available to a 76 aa long polypeptide, the initial hydrophobic collapse of the protein reduces its conformational space to $C \sim 10^{34}$, as estimated for a self-avoiding compact polymer (43). The stochastic nature of this process is demonstrated in our experiments by the fact that collapsing proteins have never been observed to follow the same path (21). However, the resulting short-lived collapsed ensemble is still incompatible with biological folding timescales. A further reduction in the number of possible configurations was predicted by simplified models to arise from attractive hydrophobic interactions between particular residues that lead to minimum energy compact structures (MECS) (11). These are thought to be a small subset with as few as 13 configurations (11, 30). An important feature of this selection process is that the conformational space remains largely independent of the length of the protein chain and occurs on millisecond timescales (11, 27). In agreement with such a folding scenario, we have discovered a population of mechanically weak but stable structures that form just milliseconds after the hydrophobic collapse.

These structures correspond to minimum energy configurations, as demonstrated by their activation energy barriers to unravel and to reach the native state. The presence of an activation barrier in the unravelling of such collapsed states is made evident by their stepwise extension under force (Fig. 3), and their Arrhenius-like force dependency (Fig. 4*B*). The slow exponential acquisition of the native state shown in Fig. 2*C* identifies the presence of an energy barrier that must be overcome to reach the native state. Although the exact number of such states is still difficult to glean from our data, their diversity is represented by a broad distribution of unraveling lengths that does not evolve with time. Even though there is a single barrier to the native basin of attraction, the rough native state of ubiquitin has been shown to exhibit a broad distribution of energies (29). It is feasible that the diversity of states sampled in the MECS gives rise to the range of native conformational energies encountered in the native state ensemble.

Lattice theories of protein folding had predicted a 3 stage ensemble folding scenario that was remarkably prescient. The existence of an ensemble of collapsed minimum energy compact structures that could interconvert into the native ensemble was a crucial prediction of these models. Our single molecule force-clamp experiments unambiguously demonstrate their existence, lending strong support to the statistical theories of protein folding.

Materials and Methods

Protein Engineering. Wt-Ubiquitin polyprotein was subcloned using the BamHI and BglII restriction sites (44). The 9-domain ubiquitin was cloned into the pQE80L (Qiagen) expression vector, and transformed into the BLR(DE3) *Escherichia coli* expression strain. PolyI27 ($I27_8$) was constructed by consecutive subcloning of the respective monomers, using the BamHI and BglII restriction sites. Constructs were purified by histidine metal-affinity chromatography with Talon resin (Clontech) and by gel-filtration, using a Superdex 200 HR column (GE Biosciences). The same procedure was used for monomer engineering (ubiquitin and I27) except for the multistep cloning step (22). The PEVK-I27 construct is based on the human titin I27 and PEVK (exon 161) sequences. The core sequence for the chimera consists of 3 tandem repeats of the PEVK exon followed by an I27 module, giving rise to the construct $(I27\text{-}PEVK_{161})_2I27$.

Force Spectroscopy. Force-clamp Atomic Force Microscopy experiments were conducted at room temperature, using a home-made set-up under force-clamp conditions described in ref. 33. The sample was prepared by depositing 1–10 μL of protein in PBS solution (at a concentration of 1–10 $\mu g \cdot mL^{-1}$ in the case of polyproteins) onto a freshly evaporated gold coverslide. Each cantilever (Si_3N_4 Veeco MLCT-AUHW) was individually calibrated using the equipartition theorm, giving rise to a typical spring constant of ≈15 pN nm^{-1}. Single proteins were picked up from the surface by pushing the cantilever onto the surface exerting a contact force of 500–800 pN so as to promote the nonspecific adhesion of the proteins on the cantilever surface. The piezoelectric actuator was then retracted to produce a set deflection (force), which was set constant throughout the experiment (≈15–30 s) thanks to an external, active feedback mechanism while the extension was recorded. The force feedback was based on a proportional, integral and differential amplifier (PID) whose output was fed to the piezoelectric positioner. The feedback response is limited to ≈3–5 ms. Thanks to the high resolution piezoelectric actuator, our measurements of protein length have a peak to peak resolution of ≈0.5 nm. Data of the force traces was filtered using a pole Bessel filter at 1 kHz. Experiments were carried out in a sodium phosphate buffer solution, specifically, 50 mM sodium phosphate (Na_2HPO_4 and NaH_2PO_4), 150 mM NaCl, pH = 7.2. Surface effects were ruled out in our experiments as described in *SI Appendix*, Figs S9 and S10.

Data Analysis. All data were recorded and analyzed using custom software written in Igor Pro 5.0 (Wavemetrics). We analyzed only recordings corresponding to the test pulse in which the protein was extended back to the full

unfolded length or that detached after a long time (≥ 6 s). We summed and normalized the test pulse trajectories of numerous (n = 30–50) recordings obtained for each particular Δt (Figs. 2 and 5) and for each particular pulling force (Fig. 4). To obtain the unfolding rate at each particular pulling force, we fitted these averaged traces with single (Fig. 4*B*) or double (Figs. 2, 4*B*, and 5) exponentials. To estimate the error on our experimentally obtained rate constants, we carried out the nonparametric bootstrap method. At a given value of force and Δt, n staircases were randomly drawn with replacement from our original dataset. These were summed and fitted to obtain a rate constant. This procedure was repeated 500 times for each dataset, resulting in a distribution that provided the standard error of the mean corresponding to the unraveling rate of the ensemble of collapsed conformations and to the unfolding rate of the native fold (Fig. 4).

ACKNOWLEDGMENTS. We thank members of the J.M.F laboratory for discussions. This work was supported by a Generalitat de Catalunya postdoctoral fellowship through the NANO and Beatriu de Pinós programs and the Fundación Caja Madrid (S.G-M.); the Burroughs Wellcome Fund (J.B.); and National Institutes of Health Grants HL66030 and HL61228 (to J.M.F).

1. Go N, Taketomi H (1978) Respective roles of short-range and long-range interactions in protein folding. *Proc Natl Acad Sci USA* 75:559–563.
2. Degennes PG (1985) Kinetics of collapse for a flexible coil. *J Phys Lett-Paris* 46:L639–L642.
3. Bryngelson JD, Wolynes PG (1987) Spin glasses and the statistical mechanics of protein folding. *Proc Natl Acad Sci USA* 84:7524–7528.
4. Bryngelson JD, wolynes PG (1989) Intermediates and barrier crossing in random energy model (with applications to protein folding). *J Phys Chem* 93:6902–6915.
5. Bryngelson JD, Wolynes PG (1990) A simple statistical field theory of heteropolymer collpase with application to protein folding. *Biopolymers* 30:177–188.
6. Baldwin RL (1994) Protein folding. Matching speed and stability. *Nature* 369:183–184.
7. Lazaridis T, Karplus M (1997) ''New view'' of protein folding reconciled with the old through multiple unfolding simulations. *Science* 278:1928–1931.
8. Onuchic JN, Wolynes PG (2004) Theory of protein folding. *Curr Opin Struct Biol* 14:70–75.
9. Brooks CL, III, Onuchic JN, Wales DJ (2001) Statistical thermodynamics. Taking a walk on a landscape. *Science* 293:612–613.
10. Sali A, Shakhnovich E, Karplus M (1994) How does a protein fold? *Nature* 369:248–251.
11. Camacho CJ, Thirumalai D (1993) Minimum energy compact structures of random sequences of heteropolymers. *Phys Rev Lett* 71:2505–2508.
12. Thirumalai D (1995) From minimal models to real proteins—Time scales for protein-folding kinetics. *J Phys I* 5:1457–1467.
13. Honeycutt JD, Thirumalai D (1990) Metastability of the folded states of globular-proteins. *Proc Natl Acad Sci USA* 87:3526–3529.
14. Yue K, Dill KA (1995) Forces of tertiary structural organization in globular-proteins. *Proc Natl Acad Sci USA* 92:146–150.
15. Dill KA, Chan HS (1997) From Levinthal to pathways to funnels. *Nat Struct Biol* 4:10–19.
16. Pande VS, Rokhsar DS (1998) Is the molten globule a third phase of proteins? *Proc Natl Acad Sci USA* 95:1490–1494.
17. Zhou YQ, Karplus M (1999) Interpreting the folding kinetics of helical proteins. *Nature* 401:400–403.
18. Went HM, Benitez-Cardoza CG, Jackson SE (2004) Is an intermediate state populated on the folding pathway of ubiquitin? *FEBS Lett* 567:333–338.
19. Crespo MD, Simpson ER, Searle MS (2006) Population of on-pathway intermediates in the folding of ubiquitin. *J Mol Biol* 360:1053–1066.
20. Fernandez JM, Li H (2004) Force-clamp spectroscopy monitors the folding trajectory of a single protein. *Science* 303:1674–1678.
21. Walther KA, et al. (2007) Signatures of hydrophobic collapse in extended proteins captured with force spectroscopy. *Proc Natl Acad Sci USA* 104:7916–7921.
22. Garcia-Manyes S, Brujic J, Badilla CL, Fernandez JM (2007) Force-clamp spectroscopy of single protein monomers reveal the individual unfolding and folding pathways of I27 and ubiquitin. *Biophys J* 93:2436–2446.
23. Fernandez JM, Li HB, Brujic J (2004) Response to comment on ''Force-clamp spectroscopy monitors the folding trajectory of a single protein.'' *Science.* 306:411C.
24. Barsegov V, Klimov DK, Thirumalai D (2006) Mapping the energy landscape of biomolecules using single molecule force correlation spectroscopy: Theory and applications. *Biophys J* 90:3827–3841.
25. Ainavarapu SR, et al. (2007) Contour length and refolding rate of a small protein controlled by engineered disulfide bonds. *Biophys J* 92:225–233.
26. Irback A, Mitternacht S, Mohanty S (2005) Dissecting the mechanical unfolding of ubiquitin. *Proc Natl Acad Sci USA* 102:13427–13432.
27. Camacho CJ, Thirumalai D (1993) Kinetics and thermodynamics of folding in model proteins. *Proc Natl Acad Sci USA* 90:6369–6372.
28. Koretke KK, Luthey-Schulten Z, Wolynes PG (1998) Self-consistently optimized energy functions for protein structure prediction by molecular dynamics. *Proc Natl Acad Sci USA* 95:2932–2937.
29. Brujic J, Hermans RI, Walther KA, Fernandez JM (2006) Single-molecule force spectroscopy reveals signatures of glassy dynamics in the energy landscape of ubiquitin. *Nat Phys* 2:282–286.
30. Thirumalai DKK (2000) *Stochastic Dynamics and Pattern Formation in Biological and Complex Systems* (American Institute of Physics, New York).
31. Labeit S, Kolmerer B (1995) Titins: Giant proteins in charge of muscle ultrastructure and elasticity. *Science* 270:293–296.
32. Li H, Linke WA, et al. (2002) Reverse engineering of the giant muscle protein titin. *Nature* 418:998–1002.
33. Schlierf M, Li H, Fernandez JM (2004) The unfolding kinetics of ubiquitin captured with single-molecule force-clamp techniques. *Proc Natl Acad Sci USA* 101:7299–7304.
34. Schuler B, Lipman EA, Eaton WA (2002) Probing the free-energy surface for protein folding with single-molecule fluorescence spectroscopy. *Nature* 419:743–747.
35. Dudko OK, Hummer G, Szabo (2006) A Intrinsic rates and activation free energies from single-molecule pulling experiments. *Phys Rev Lett* 96:108101.
36. Lipman EA, Schuler B, Bakajin O, Eaton WA (2003) Single-molecule measurement of protein folding kinetics. *Science* 301:1233–1235.
37. Schuler B, Eaton WA (2008) Protein folding studied by single-molecule FRET. *Curr Opin Struct Biol* 18:16–26.
38. Rhoades E, Gussakovsky E, Haran G (2003) Watching proteins fold one molecule at a time. *Proc Natl Acad Sci USA* 100:3197–3202.
39. Schlierf M, Berkemeier F, Rief M (2007) Direct observation of active protein folding using lock-in force spectroscopy. *Biophys J* 93:3989–3998.
40. Cecconi C, Shank EA, Bustamante C, Marqusee S (2005) Direct observation of the three-state folding of a single protein molecule. *Science* 309:2057–2060.
41. Kuwajima K (1989) The molten globule state as a clue for understanding the folding and cooperativity of globular-protein structure. *Proteins* 6:87–103.
42. Ptitsyn OB, Pain RH, Semisotnov GV, Zerovnik E, Razgulyaev OI (1990) Evidence for a molten globule state as a general intermediate in protein folding. *FEBS Lett* 262:20–24.
43. Fisher ME, Hiley BJ (1961) Configuration and free energy of a polymer mole with solvent interaction. *J Chem Phys* 34:1253.
44. Carrion-Vazquez M, et al. (1999) Mechanical and chemical unfolding of a single protein: A comparison. *Proc Natl Acad Sci USA* 96:3694–3699.
45. Brujic J, Hermans RI, Garcia-Manyes S, Walther KA, Fernandez JM (2007) Dwell-time distribution analysis of polyprotein unfolding using force-clamp spectroscopy. *Biophys J* 92:2896–2903.